Title

Inhibition of EGFR Signaling Protects from Mucormycosis

Journal

mBio, 9(4)

ISSN

2161-2129

Authors

Watkins, Tonya N
Gebremariam, Teclegiorgis
Swidergall, Marc
et al.

Publication Date

2018-09-05

DOI

10.1128/mbio.01384-18

AMERICAN SOCIETY FOR MICROBIOLOGY | mBio®

RESEARCH ARTICLE

Inhibition of EGFR Signaling Protects from Mucormycosis

Tonya N. Watkins,[a] Teclegiorgis Gebremariam,[b] Marc Swidergall,[b] Amol C. Shetty,[a] Karen T. Graf,[a] Abdullah Alqarihi,[b] Sondus Alkhazraji,[b] Abrar I. Alsaadi,[b] Vonetta L. Edwards,[a] Scott G. Filler,[b,c] Ashraf S. Ibrahim,[b,c] Vincent M. Bruno[a,d]

[a]Institute for Genome Sciences, University of Maryland School of Medicine, Baltimore, Maryland, USA

[b]Division of Infectious Diseases, Los Angeles Biomedical Research Institute at Harbor, UCLA Medical Center, Torrance, California, USA

[c]David Geffen School of Medicine at UCLA, Torrance, California, USA

[d]Department of Microbiology and Immunology, University of Maryland School of Medicine, Baltimore, Maryland, USA

ABSTRACT Mucormycosis is a life-threatening, invasive fungal infection that is caused by various species belonging to the order Mucorales. *Rhizopus* species are the most common cause of the disease, responsible for approximately 70% of all cases of mucormycosis. During pulmonary mucormycosis, inhaled *Rhizopus* spores must adhere to and invade airway epithelial cells in order to establish infection. The molecular mechanisms that govern this interaction are poorly understood. We performed an unbiased survey of the host transcriptional response during early stages of *Rhizopus arrhizus* var. *delemar* (*R. delemar*) infection in a murine model of pulmonary mucormycosis using transcriptome sequencing (RNA-seq). Network analysis revealed activation of the host's epidermal growth factor receptor (EGFR) signaling. Consistent with the RNA-seq results, EGFR became phosphorylated upon *in vitro* infection of human alveolar epithelial cells with several members of the Mucorales, and this phosphorylated, activated form of EGFR colocalized with *R. delemar* spores. Inhibition of EGFR signaling with cetuximab or gefitinib, specific FDA-approved inhibitors of EGFR, significantly reduced the ability of *R. delemar* to invade and damage airway epithelial cells. Furthermore, gefitinib treatment significantly prolonged survival of mice with pulmonary mucormycosis, reduced tissue fungal burden, and attenuated the activation of EGFR in response to pulmonary mucormycosis. These results indicate EGFR represents a novel host target to block invasion of alveolar epithelial cells by *R. delemar*, and inhibition of EGFR signaling provides a novel approach for treating mucormycosis by repurposing an FDA-approved drug.

IMPORTANCE Mucormycosis is an increasingly common, highly lethal fungal infection with very limited treatment options. Using a combination of *in vivo* animal models, transcriptomics, cell biology, and pharmacological approaches, we have demonstrated that Mucorales fungi activate EGFR signaling to induce fungal uptake into airway epithelial cells. Inhibition of EGFR signaling with existing FDA-approved drugs significantly increased survival following *R. arrhizus* var. *delemar* infection in mice. This study enhances our understanding of how Mucorales fungi invade host cells during the establishment of pulmonary mucormycosis and provides a proof-of-concept for the repurposing of FDA-approved drugs that target EGFR function.

KEYWORDS EGFR, gefitinib, *Rhizopus*, mucormycosis

Mucormycosis is an invasive fungal infection of humans caused by species of the order Mucorales, subphylum Mucormycotina (1, 2). *Rhizopus* spp. are the most common etiologic agent of mucormycosis and are responsible for approximately 70% of all cases (1–3). The primary risk factors for mucormycosis include neutropenia, diabetes mellitus resulting in hyperglycemia and diabetic ketoacidosis (DKA), solid

Received 25 June 2018 **Accepted** 20 July 2018 **Published** 14 August 2018

Citation Watkins TN, Gebremariam T, Swidergall M, Shetty AC, Graf KT, Alqarihi A, Alkhazraji S, Alsaadi AI, Edwards VL, Filler SG, Ibrahim AS, Bruno VM. 2018. Inhibition of EGFR signaling protects from mucormycosis. mBio 9:e01384-18. https://doi.org/10.1128/mBio.01384-18.

Invited Editor Robert T. Wheeler, University of Maine

Editor Michael Lorenz, University of Texas Health Science Center

Address correspondence to Vincent M. Bruno, vbruno@som.umaryland.edu.

organ or bone marrow transplantation, treatment with corticosteroids, deferoxamine therapy, trauma and burns (e.g., wounded soldiers in combat), and malignant hematological disorders (2, 4).

The most common forms of mucormycosis, based on anatomical site, are rhino-orbital/cerebral, pulmonary, cutaneous, gastrointestinal, and disseminated. Rhino-orbital/cerebral mucormycosis is found almost exclusively in DKA patients, while pulmonary disease is mainly found in neutropenic patients (5). Cutaneous necrotizing mucormycosis outbreaks in healthy individuals have also been reported and often follow natural disasters or severe trauma (e.g., infections following the tsunami that devastated Southeast Asia in 2004 and the tornadoes that occurred in Joplin, MO, in June 2011) (6, 7). Since there are no federal requirements to report fungal infections, the true prevalence of mucormycosis is likely to be much higher than currently reported.

There are very few antifungal agents approved by the United States FDA for treating mucormycosis; the first is amphotericin B (AmB), which has been used to treat mucormycosis for the last 6 decades. AmB has significant nephrotoxicity, other adverse effects, and very limited clinical success (2, 8). Although isavuconazole and posaconazole have been recently approved to treat mucormycosis, neither is considered to be superior to AmB treatment (8, 9). In the absence of surgical removal of the infected focus (for example, excision of the eye in patients with rhinocerebral mucormycosis), antifungal therapy alone is rarely curative. Even when surgical debridement is combined with high-dose antifungal therapy, the mortality associated with mucormycosis is >50%. In patients with prolonged neutropenia or disseminated disease, mortality is 90 to 100% (10, 11). The limited treatment options coupled with the high mortality and morbidity rates and the frequently disfiguring surgical therapy provide a clear mandate to explore alternative approaches to treat this infection.

In the case of pulmonary mucormycosis, infection is generally acquired by inhalation of spores that are ubiquitous in nature. As lung epithelial cells are among the first host cells that interact with Mucorales spores during pulmonary infection, a molecular understanding of how these cells sense and respond to the pathogen is essential to understanding the pathogenesis of pulmonary mucormycosis. While the invasion of endothelial cells by *Rhizopus arrhizus* var. *delemar* (referred to from here on as *R. delemar*) is known to be mediated by the interaction between the fungus-encoded CotH3 and the host-encoded GRP78 (12, 13), the specific interactions that govern adherence and invasion of lung epithelial cells are poorly understood.

In this study, we used transcriptome sequencing (RNA-seq) to examine the host transcriptional response to *R. delemar* infection in a well-established *in vivo* murine model of pulmonary mucormycosis. Network analysis of the data set revealed the modulation of host pathways that were not previously linked to the host response to mucormycosis. We provide evidence that the epidermal growth factor receptor (EGFR) pathway is activated by *R. delemar* and other Mucorales infection and that this activation mediates invasion of lung epithelial cells by these fungi. Importantly, gefitinib, an FDA-approved drug that inhibits EGFR, protected mice from mucormycosis. These results suggest that inhibition of EGFR signaling provides a novel therapeutic approach for treating mucormycosis.

RESULTS

RNA-seq analysis of a murine model of mucormycosis. We analyzed the host transcriptional response to *R. delemar* in a DKA murine model of pulmonary mucormycosis due to *R. delemar* infection. At 14 and 24 h postinoculation, animals were sacrificed, and the lungs were harvested for extraction of total RNA for subsequent transcriptome analysis using RNA-seq. These time points were chosen because they represent early stages of infection, prior to the onset of massive tissue damage and necrosis, which might complicate interpretation of transcriptome analyses. The early time points also allowed us to focus on the initial response of the lung tissue during adhesion of spores to and subsequent invasion of the airway epithelium. From each of

the 12 sequencing libraries, we obtained an average of 96.4 ± 15.8 million reads that mapped to the mouse reference genome (see Table S1 in the supplemental material). The inclusion of a poly(A) enrichment step in the RNA-seq protocol, as predicted, resulted in the detection of transcripts from the infecting fungus. However, a robust analysis of the *R. delemar* transcriptome was precluded by the lack of sufficient reads that mapped to the *R. delemar* reference genome (6,488 reads combined from all six infected samples). Therefore, we focused our analysis of these samples on the host response.

We have previously demonstrated that infection-induced transcriptome changes can be used to identify signaling pathways that govern the interaction between host and fungal pathogen (14–16). Using the Ingenuity Pathway Analysis (IPA) software (Ingenuity Systems; http://www.ingenuity.com), we performed an upstream regulator analysis on the sets of host genes that were differentially expressed ($P < 0.05$) (see Tables S2 and S3 in the supplemental material) between the infection groups and the appropriate time-matched negative-control groups, which were immunosuppressed but not infected.

This approach was validated by our identification of two pathways that were already linked to infection by Mucorales: interleukin-22 (IL-22) and IL-17A (Fig. 1A) (17). Our analysis also predicted the activation of signaling pathways that have not been tied to mucormycosis but have been associated with the host response to fungal infection, including colony-stimulating factor 2 (CSF2), extracellular signal-regulated kinases (ERKs), myeloid differentiation primary response 88 (MYD88), and JNK (Jun N-terminal kinase) (18–24) (Fig. 1A). We also noticed a striking temporal dynamic in our data set. Specifically, the majority of the pathways are modulated at 14 h postinoculation (hpi) and returning to normal 24 h postinfection. Furthermore, a smaller subset of pathways was modulated only at 24 h postinfection.

Of particular interest was the significant overlap between genes that are differentially expressed 14 h postinoculation with *R. delemar* and the known transcriptional targets of the epidermal growth factor receptor (EGFR) signaling pathway (*P* value of overlap, 9.57×10^{-6}). Specifically, *R. delemar* infection induced the expression of 18 genes that are known to be activated by EGFR signaling (Fig. 1B), providing evidence for the activation of EGFR protein in response to *R. delemar* infection.

Further support of the activation of EGFR signaling was provided by the predicted activation of mir-21 (*P* value overlap, 8.6×10^{-15} [Fig. 1A]), a microRNA that governs the expression of genes involved in many different biological processes (25–30). EGFR activation enhances the expression of mir-21 in lung epithelial cells (31). Our sequencing approach, which is geared toward the detection of long transcripts, does not allow the examination of microRNAs. However, in our infection model, 28 known repression targets and 5 known activation targets of mir-21 were downregulated or upregulated, respectively, 14 h after inoculation relative to the uninfected control group (see Table S4 in the supplemental material). This downregulation of mir-21-repressed genes is consistent with an EGFR-stimulated increase in mir-21 expression. In the database used to perform the upstream regulator analysis, none of the 33 mir-21 target genes are annotated as EGFR targets, and they are therefore not included in Fig. 1C, so the total number of differentially expressed genes that provide evidence of EGFR pathway activation is 51.

EGFR signaling is activated during *in vitro* infection of airway epithelial cells. We have previously examined the transcriptional response of A549 human alveolar epithelial cells to infection with *R. delemar* at 6 and 16 h (15). Upstream regulator analysis of this *in vitro* RNA-seq data set also revealed a significant overlap between genes that are differentially expressed following *R. delemar* infection and the known transcriptional targets of the EGFR signaling pathway (*P* values of 4.33×10^{-2} and 1.43×10^{-3} for 6 and 16 h, respectively). Specifically, *R. delemar* infection induced changes in gene expression of 34 known downstream targets of EGFR signaling in a direction that is consistent with the activation of the EGFR (29 activated and 5 repressed [Fig. 1C]).

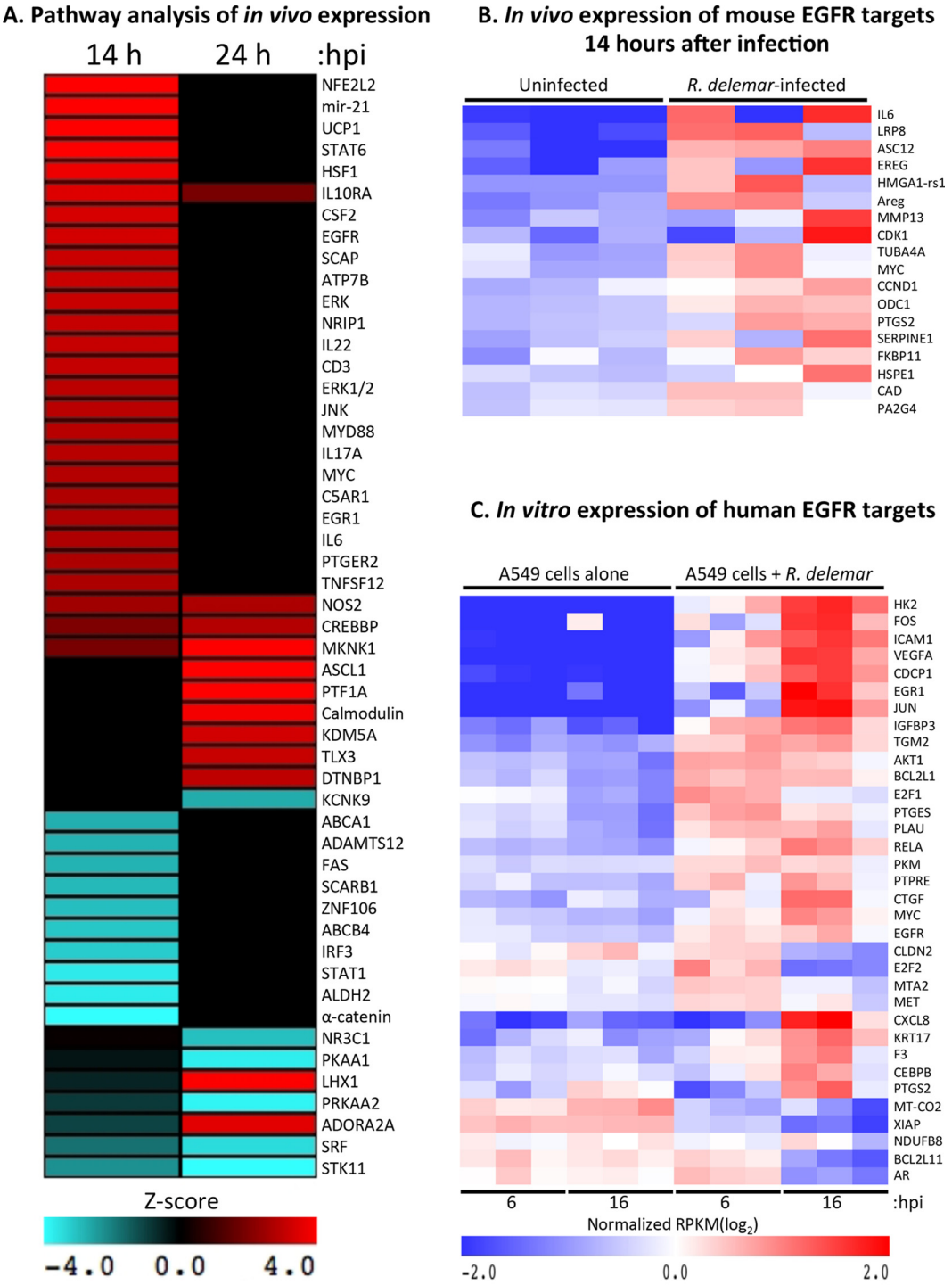

FIG 1 Host response to *R. delemar* infection *in vivo* and *in vitro*. (A) Mouse upstream regulators that are predicted to be changed in *R. delemar*-infected lungs in a mouse DKA model of mucormycosis. Red indicates predicted activation (*Z* score of >2). Teal indicates predicted repression (*Z* score of < −2). Black indicates no predicted effect. (B) Expression of known mouse EGFR targets in lungs 14 h postinoculation of the *in vivo* DKA model. (C) Expression of known human EGFR targets in A549 cells at 6 and 16 h following inoculation of an *in vitro* infection. Plotted for panels B and C are the log-transformed reads per kilobase per million (RPKM) values that have been normalized across all samples. Red indicates high gene expression; blue indicates low expression. Each column in panels B and C represents an individual sample from a different mouse.

When EGFR is activated by ligand binding, tyrosine residues at the intracellular carboxy terminus become phosphorylated and the signal is transmitted to a variety of downstream signaling pathways (32). To confirm the EGFR activation by an orthogonal approach, we tested whether *R. delemar* infection of the A549 pulmonary epithelial cell

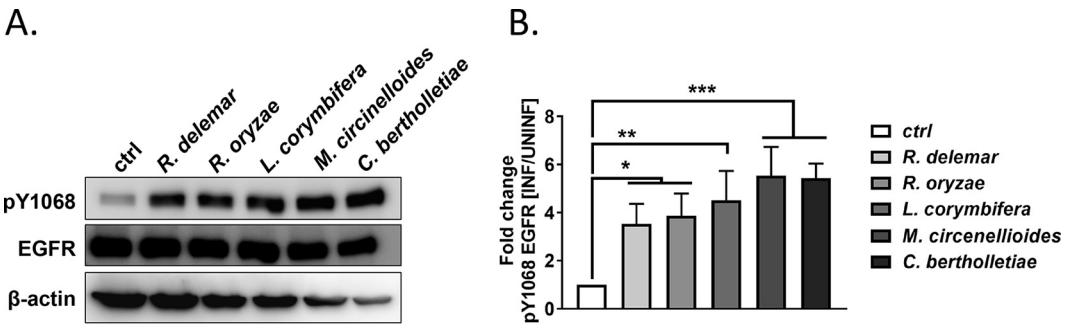

FIG 2 Phosphorylation and localization of EGFR in A549 cells infected with Mucorales. (A) Representative immunoblot examining tyrosine phosphorylation of EGFR residue Y1068 in response to individual infection with five different Mucorales fungi. (B) Densitometric analysis of the immunoblots. ctrl, control.

line stimulated the phosphorylation of EGFR by immunoblotting. *R. delemar* infection induced the phosphorylation of EGFR on tyrosine residue 1068 when examined 3 h postinfection (Fig. 2). The same phosphorylation was also induced following infection with four other Mucorales species—*Rhizopus oryzae*, *Lichtheimia corymbifera*, *Mucor circinelloides*, and *Cunninghamella bertholletiae* (Fig. 2)—indicating that EGFR activation is not a strain- or species-specific phenomenon. Consistent with these results, we observed that the phosphorylated (activated) form of EFGR colocalized with *R. delemar* spores during *in vitro* infection of A549 cells (Fig. 3). We did not observe colocalization when *R. delemar* spores were examined in the absence of A549 cells (see Fig. S1 in the supplemental material). Taken together, these results are consistent with a model in which Mucorales interacts with EGFR and activates signaling in airway epithelial cells.

EGFR signaling governs the uptake of Mucorales and subsequent damage of airway epithelial cells. The predicted activation of EGFR and mir-21 signaling early during the infection process, the colocalization of activated EGFR with *R. delemar*, and the involvement of EGFR in invasion by *Candida albicans* and diverse microbial pathogens (33–35) compelled us to explore the possibility that EGFR mediates the invasion of airway epithelial cells by *R. delemar*. Thus, we next tested whether blocking EGFR signaling would protect alveolar epithelial cells from invasion by *R. delemar*. We used gefitinib, a clinically relevant EGFR kinase inhibitor, to study its effect on *R. delemar*-mediated endocytosis by alveolar epithelial cells and their subsequent damage. When A549 cells were pretreated for 1 h with 25 μM gefitinib, endocytosis of *R. delemar* spores was significantly reduced compared to pretreatment with vehicle alone (Fig. 4A).

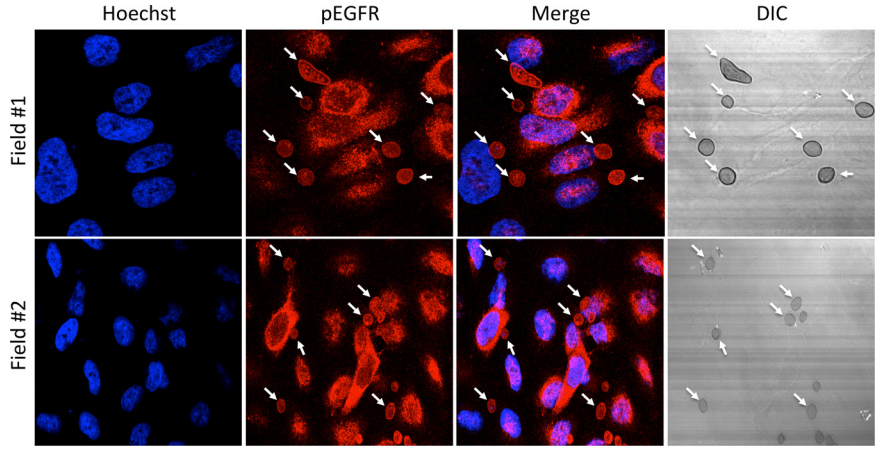

FIG 3 Localization of phosphor-EGFR in A549 cells infected with *R. delemar*. A549 cells were infected for 30 min with 2×10^5 *R. delemar* spores that had been germinated for 1 h. Cells were then stained for phospho-EGFR (red) and host cell nuclei using Hoechst (blue). DIC, differential inference contrast.

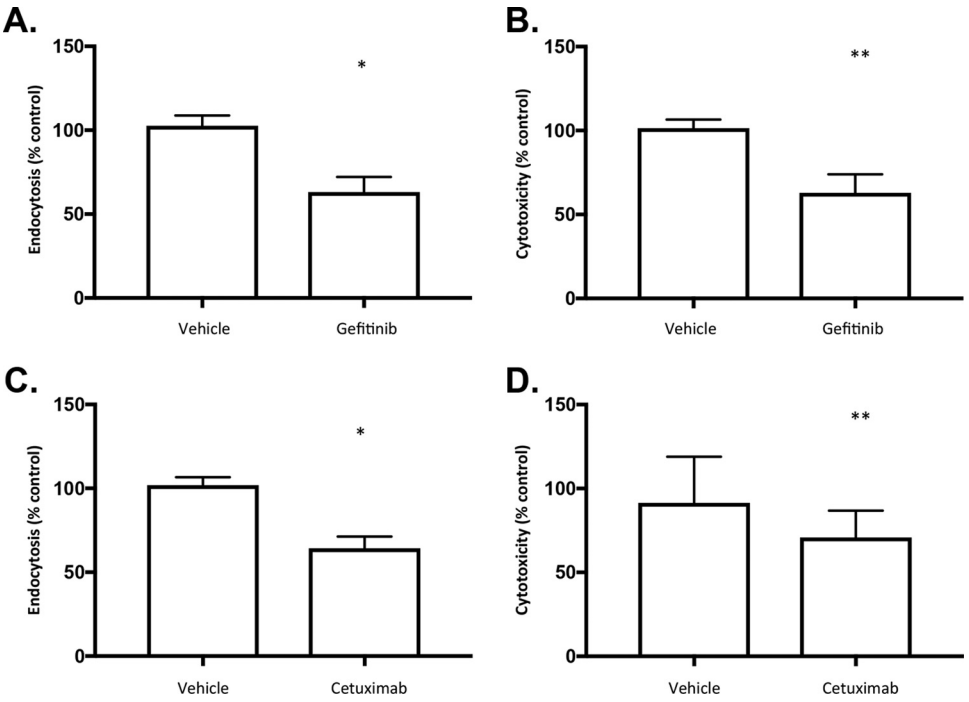

FIG 4 Effects of EGFR inhibition on invasion of airway epithelial cells by *R. delemar*. A549 alveolar epithelial cells were pretreated with vehicle, 25 μM gefitinib, or 25 μg/ml cetuximab for 1 h followed by (top) 3 h of infection in the presence of inhibitor with 2×10^5 *R. delemar* spores or (bottom) 24 h of infection (in the presence of inhibitors) with 2×10^6 *R. delemar* spores that were germinated for 1 h. *, $P < 0.0001$, and **, $P < 0.01$, versus control by Wilcoxon rank-sum test. Data are expressed as median ± interquartile range and represent at least two independent experiments.

Pretreatment with gefitinib also significantly reduced *R. delemar*-induced damage of A549 cells, when assayed by lactate dehydrogenase (LDH) assay (Fig. 4B).

To complement our studies with gefitinib, which targets the intracellular tyrosine kinase domain of EGFR, we examined the ability of cetuximab to block epithelial cell invasion. Cetuximab is a monoclonal antibody that recognizes the extracellular portion of EGFR and has been shown to block ligand-dependent activation of EGFR signaling (36). When the same host cells were pretreated for 1 h with 25 μg/ml cetuximab, endocytosis of *R. delemar* spores and host cell damage were both significantly reduced compared to pretreatment with an equivalent amount of IgG1 control antibody (Fig. 4C and D). Notably, neither gefitinib nor cetuximab inhibited *R. delemar* mycelial growth (see Fig. S2 in the supplemental material). Pretreatment of *R. delemar* spore preparations with gefitinib or cetuximab, followed by rinsing, prior to the infection did not reduce endocytosis or host cell damage (see Fig. S3 in the supplemental material). The concordance between the results of the endocytosis assay and the host cell damage assay is consistent with previous observations that endocytosis of *R. delemar* is a prerequisite for inducing host cell damage of endothelial cells (37). We also found that pretreatment with gefitinib reduced fungus-induced damage of A549 cells following infection with *R. oryzae*, *L. corymbifera*, *M. circinelloides*, and *C. bertholletiae* (Fig. 5). Collectively, these results indicate that EGFR signaling is required for maximal invasion of and damage to alveolar epithelial cells by Mucorales.

EGFR signaling has also been shown to facilitate invasion of oral epithelial cells by *C. albicans* which, like *R. delemar*, enters cells by induced endocytosis. The EGFR-dependent invasion of *C. albicans* requires the activation of the aryl hydrocarbon receptor (Ahr) and the subsequent activation of Src family kinases, which in turn phosphorylate and activate EGFR (34, 38). To address whether the same mechanism is being employed to facilitate invasion of airway epithelial cells by *R. delemar*, we measured the effect of an Ahr inhibitor (CH-223191) and an Src inhibitor (Src kinase

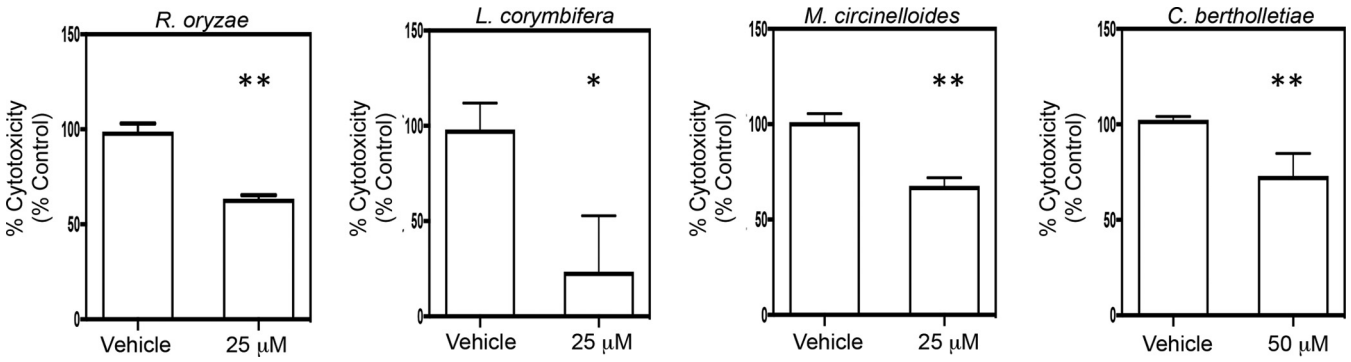

FIG 5 Gefitinib inhibits infection-induced damage of airway epithelial cells by four different species of Mucorales. A549 alveolar epithelial cells were pretreated with vehicle or gefitinib (25 or 50 μM) for 1 to 2 h followed by 24 h of infection (in the presence of inhibitors) with 2×10^6 (*C. bertholletiae* and *R. oryzae*) or 3×10^6 (*L. corymbifera* and *M. circineollides*) spores that were germinated for 1 h *, $P < 0.0001$, and **, $P < 0.01$, versus the control by Wilcoxon rank sum test. Data are expressed as median ± interquartile range and represent at least two independent experiments done in triplicate.

inhibitor II) on endocytosis. Neither of the inhibitors altered the ability of A549 cells to endocytose *R. delemar* spores (see Fig. S4 in the supplemental material). These results suggest that the mechanism of activation of EGFR in epithelial cells is distinct from the activation of EGFR by *C. albicans*.

Gefitinib treatment increases survival of mice with mucormycosis. We next sought to determine if EGFR signaling governs the establishment and/or progression of mucormycosis in a well-established *in vivo* murine model of mucormycosis. Unfortunately, mice harboring deletions in EGFR die within the first 8 days of life (39), thus precluding our ability to test the receptor in a traditional mouse gene deletion experiment. Furthermore, there are no published lung-specific deletion models for EGFR. Therefore, we infected neutropenic mice intratracheally with *R. delemar* (40) and treated them with 10 mg/kg of body weight gefitinib (41) or vehicle alone (placebo) for 5 consecutive days starting 4 h postinfection. We chose to begin the intervention at 4 h because invasion of lung epithelial cells is an early event in the infection. Placebo-treated mice had a median survival time of 8 days and 85% mortality by day 15 postinfection (Fig. 6A). In contrast, mice treated with gefitinib had a median survival time of >21 days, and 55% of the mice remained alive by day 21, when the experiment was terminated, and the surviving mice appearing healthy. Corroborating the effects of gefitinib on survival, mice treated with this drug had an ~1-log reduction in their lungs and brains relative to placebo-treated mice (Fig. 6B). Consistent with these results, we found that infection with *R. delemar* induced marked tyrosine phosphorylation of EGFR in the lung (Fig. 6C) and that treatment of mice with gefitinib significantly reduced this phosphorylation (Fig. 6C). These results validate our *in vitro* observations and support the potential of targeting EGFR signaling as a novel therapeutic strategy for mucormycosis by immediately repurposing currently FDA-approved cancer drugs.

DISCUSSION

Invasion of the airway epithelium is a crucial, yet poorly understood, step in the initiation of pulmonary mucormycosis. We took an unbiased approach to understand the host side of this interaction by performing RNA-seq analysis of infected lungs harvested during early stages of a well-established clinically relevant murine model of mucormycosis. A network analysis of differential gene expression in these mice revealed the enrichment for genes that are known to be downstream of EGFR and its regulatory target, mir-21. Because our analysis was performed on RNA harvested from whole lungs of infected mice, we were unable to determine which cell types responded to the infection with the increased gene expression. The predicted activation of EGFR signaling at 14 h, and not 24 h, could be indicative of a host response to the early stage of infection when *R. delemar* first invades the airway epithelium. Our *in vitro* analyses

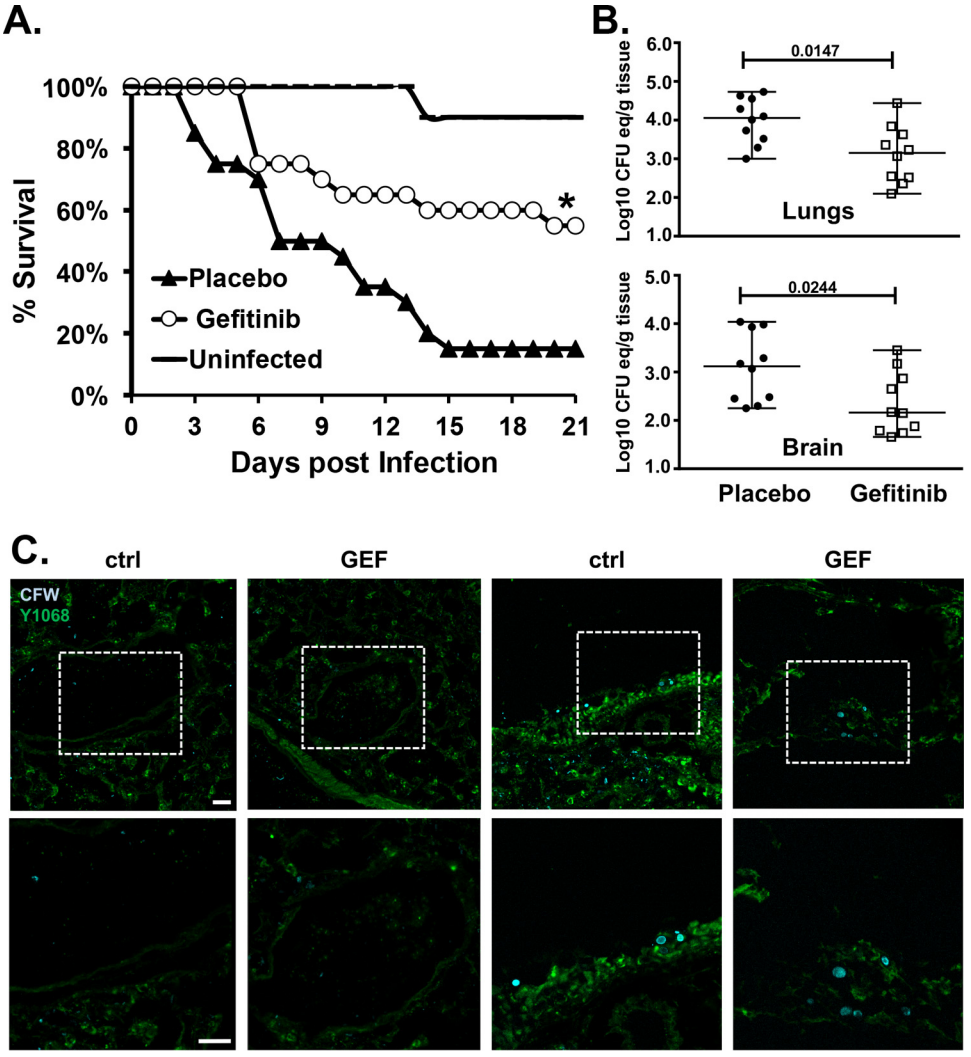

FIG 6 Gefitinib inhibits EGFR phosphorylation *in vivo* and protects mice from pulmonary mucormycosis. (A) Survival of neutropenic mice ($n = 20$/group from two independent experiments with similar results) infected intratracheally with *R. delemar* (average inoculum of 3.8×10^3 spores per mouse) and treated with vehicle control (placebo) or 10 mg/kg gefitinib 4 h postinfection for 5 consecutive days. *, $P = 0.0084$ versus placebo-treated mice by log rank test. (B) Tissue fungal burden of lungs and brains of mice ($n = 10$ per group) infected intratracheally with *R. delemar* (5.6×10^3 spores per mouse of confirmed inoculum) and treated with vehicle control (placebo) or gefitinib. Data are presented as median ± interquartile range. (C) Twenty-four hours post-intratracheal infection, lungs of gefitinib (GEF)-treated or untreated mice were harvested, sectioned, and stained with calcofluor white (CFW) and anti-pY1068 antibody. Scale bars, 20 μm. Dashed boxes in the top row of panels indicate the sections shown enlarged in the bottom row. ctrl, control.

of human airway epithelial (A549) cells support this idea. Specifically, 34 EGFR-responsive genes are modulated during infection with *R. delemar*, and phospho-EGFR colocalized with endocytosed spores. Furthermore, pharmacological inhibition of EGFR signaling reduced both fungus-induced cytotoxicity and endocytosis of the spores by the A549 cells. Collectively, these results suggest that EGFR signaling mediates the invasion of airway epithelial cells by *R. delemar*. Hence, EGFR is the first host cell receptor to be implicated in the interaction between *R. delemar* and airway epithelial cells.

In general, EGFR signaling can be activated by binding to any one of seven known host-derived ligands, all of which are expressed as precursor proteins that span the plasma membrane and are cleaved by cell surface proteases upon stimulation (42). Upon cleavage, the extracellular domains are released as mature proteins into the extracellular space, where they can bind to and activate EGFR on the surface of the

same cells or on adjacent cells (42). In addition, many pathogens, including viruses, bacteria, and fungi, seem to have evolved the ability to exploit EGFR signaling to gain entry into host cells (33), and the mechanism of EGFR activation across these pathogenic microbes varies. For example, in the context of viral infection, hepatitis C virus increases signaling by disrupting EGFR recycling to enhance its surface expression (43, 44). In contrast, the *Campylobacter jejuni* bacterium induces lipid raft formation, resulting in clustering and subsequent activation of EGFR (45), while meningitic *Escherichia coli* activates EGFR signaling by increasing sphingosine 1-phosphate ($S1P_2$)-dependent release of heparin-binding ligand-like epidermal growth factor (HB-EGF) (35). The fungal pathogen *C. albicans* expresses two surface proteins, Als3p and Ssa1p, that likely bind to and activate EGFR and ErbB2 heterodimers (34).

At this point, we do not know the molecular mechanism by which EGFR signaling is being stimulated during *R. delemar* infection. The colocalization of EGFR with fungal spores is consistent with an interaction between a fungal cell wall component and EGFR. The invasion of A549 cells by an *R. delemar* strain with attenuated expression of CotH3 (12), the Mucorales ligand to host GRP78 during interaction with human umbilical vein endothelial cells, was not different from A549 cell invasion caused by wild-type *R. delemar* (Ashraf Ibrahim, unpublished data). Thus, CotH3 protein is not the fungal ligand by which EGFR is activated. Furthermore, the *R. delemar* genome does not encode a recognizable ortholog of *ALS3* or *SSA1* and inhibition of Src kinase activity or Ahr does not inhibit *R. delemar* invasion, suggesting that EGFR stimulation by Mucorales occurs via a different mechanism than that by *C. albicans*. Further experiments are required to determine the molecular nature of the activation.

Our *in vitro* blocking data using EGFR inhibitors did not entirely abrogate the ability of *R. delemar* to invade and damage alveolar epithelial cells. This strongly indicates that receptors other than EGFR are involved in the interaction of *Rhizopus* with these host cells. We have previously identified a host cell receptor, GRP78, required for *R. delemar* hematogenous dissemination. Specifically, the host 78-kDa glucose-regulated protein GRP78 interacts with the Mucorales-specific CotH3 cell wall protein during invasion of human umbilical vein endothelial cells (12). Because of the lack of CotH3 contribution to invasion of A549 cells (Ibrahim, unpublished), it is unlikely that GRP78 acts as a coreceptor with EGFR during interactions with invading Mucorales. Alternatively, GRP78 could contribute to Mucorales invasion of alveolar epithelial cells through interacting with a fungal ligand(s) other than CotH3. These possibilities are the topic of active investigation.

Since EGFR plays a central role in the progression of several types of cancer, significant effort has been put forth into developing therapies that target EGFR function (46). To this end, gefitinib, a small molecular inhibitor of EGFR kinase activity, and cetuximab, a monoclonal antibody specific for the extracellular domain of EGFR, provide valuable tools to test the role of EGFR in epithelial cell invasion by *R. delemar*. Indeed, in our mouse model of mucormycosis, treatment with gefitinib significantly increased survival and reduced tissue fungal burden of target organs. These results are consistent with a model in which *R. delemar* stimulates EGFR signaling *in vivo* to facilitate endocytosis of the fungus by airway epithelial cells and raise the exciting possibility of repurposing an FDA-approved drug to potentially control these invasive fungal infections. Since immunocompromised patients are the most susceptible and likely to develop mucormycosis, the observed efficacy of gefitinib in neutropenic mice adds to the clinical relevance and the potential for our results to translate to humans as an adjunctive therapy to current antifungal agents. Furthermore, because gefitinib targets the host and does not affect the growth or morphology of the fungus, acquisition of resistance is less likely to occur.

To summarize, we have identified host EGFR as a key mediator of early invasion of alveolar epithelial cells by Mucorales. Of great clinical importance is our finding that inhibition of EGFR function by an FDA-approved drug ameliorates murine mucormycosis and is likely to represent a new therapeutic modality as adjunctive therapy to lethal mucormycosis.

MATERIALS AND METHODS

Fungal strains and host cells. *R. delemar* strain 99-880 (a clinical isolate obtained from a patient with rhino-orbital mucormycosis), *R. oryzae* strain 99-892, *L. corymbifera* strain 008-049, *M. circinelloides* strain NRRL3631, and *C. bertholletiae* strain 175 were grown on peptone-dextrose agar (PDA) plates for 3 to 5 days at 37°C. Spores were collected in endotoxin-free Dulbecco's phosphate-buffered saline (DPBS), washed with endotoxin-free DPBS, and counted with a hemocytometer to prepare the final inocula. To form germlings, spores were incubated in yeast extract-peptone-dextrose (YPD) with shaking for 1 h at 37°C. Germlings were washed twice with endotoxin-free DPBS. The A549 type II pneumocyte cell line was grown in tissue culture dishes in F-12K medium with L-glutamine plus 10% fetal bovine serum (FBS).

Drug. Src kinase inhibitor II (CAS 459848-35-2; Calbiochem) was obtained from Millipore (catalog no. 567806).

Murine models of mucormycosis. For the *in vivo* RNA-seq experiments, diabetic ketoacidosis (DKA) was induced and mice were infected intratracheally with a target inoculum of 2.5×10^5 fungal spores of *R. delemar* 99-880 in 25 μl as previously described (12). To test the effect of gefitinib on mouse survival following infection, male ICR mice (20 to 25 g [from Envigo]) were immunosuppressed by cyclophosphamide (200 mg/kg administered intraperitoneally [i.p.]) and cortisone acetate (500 mg/kg administered subcutaneously) given on days -2, $+3$, and $+9$ relative to infection. This treatment resulted in 16 days of pancytopenia (40). To control for bacterial infection, immunosuppressed mice received 50 mg/liter enrofloxacin (Baytril; Bayer, Leverkusen, Germany) *ad libitum* on day -3 through day 0, after which the enrofloxacin was replaced with daily ceftazidime (5 mg/mouse) treatment administered subcutaneously through day $+13$ relative to infection. Mice were infected with 2.5×10^5 spores of *R. delemar* 99-880 in 25 μl PBS given intratracheally as previously described (40). Treatment with gefitinib (10 mg/kg dissolved in 10% dimethylacetamide–90% polyethylene glycol 300 [DMA-PEG 300] and administered i.p.) started 4 h postinfection and continued once daily through day $+4$. Placebo-treated mice received DMA-PEG 300. Survival of mice served as the primary endpoint, with moribund mice humanely euthanized. To determine the effect of treatment on tissue fungal burden, mice were immunosuppressed and infected as described above. Gefitinib treatment started 4 h postinfection and continued through day $+3$. On day $+4$, mice were sacrificed, and lungs and brains, representing primary and secondary target organs (40), were collected and processed for tissue fungal burden by quantitative PCR (qPCR) (47). Values are expressed as $\log_{10}$ spore equivalents per gram of tissue.

All animal studies were approved by the Institutional Animal Care and Use Committee (IACUC) of the Los Angeles Biomedical Research Institute at Harbor-UCLA Medical Center according to the NIH guidelines for animal housing and care (approval reference no. 21125).

Isolation of RNA from lung tissue. Male ICR mice were immunosuppressed and infected as described above. Lungs were harvested 14 or 24 h postinfection and flash frozen in liquid nitrogen prior to extracting total RNA using Tri reagent solution (Ambion).

RNA-seq and gene expression analysis. Our deep sequencing analysis was performed in triplicate with three lungs per group isolated from 3 different mice. Sequencing libraries (non-strand-specific, paired end) were prepared with the TruSeq RNA sample prep kit (Illumina). The total RNA samples were subjected to poly(A) enrichment as part of the TruSeq protocol. One hundred fifty nucleotides of sequence was determined from both ends of each cDNA fragment using the HiSeq platform (Illumina) per the manufacturer's protocol. Sequencing reads were annotated and aligned to the UCSC mouse reference genome (mm10, GRCm38.75) using TopHat2 (48). The alignment files from TopHat2 were used to generate read counts for each gene, and a statistical analysis of differential gene expression was performed using the edgeR package from Bioconductor (49). A gene was considered differentially expressed if the *P* value for differential expression was less than 0.05. To identify modulated signal transduction pathways, we used the upstream regulator analytic of IPA (Ingenuity Systems) to identify signaling proteins that are potentially activated or repressed during the course of infection. This analysis determines the overlap between lists of differentially expressed genes and an extensively curated database of regulator-target gene relationships. It then considers the direction of the gene expression changes to make predictions about activation or repression of specific pathways.

Immunoblot of EGFR phosphorylation *in vitro*. The A549 type II pneumocyte cell line (American Type Culture Collection) was grown as described previously (50). A549 cells in 24-well tissue culture plates were incubated in F-12K tissue culture medium supplemented with fetal bovine serum to a final concentration of 10%. Prior to infection, the A549 cells were serum starved for 120 min. Spores of *R. delemar*, *R. oryzae*, *L. corymbifera*, *M. circinelloides*, or *C. bertholletiae* were incubated in RPMI for 60 min at 37C, washed, and suspended in F-12K medium. A549 cells were infected for 3 h with a multiplicity of infection (MOI) of 5. Next, the cells were rinsed with cold Hanks balanced salt solution (HBSS) containing protease and phosphatase inhibitors and removed from the plate with a cell scraper. After collecting the cells by centrifugation, they were boiled in 2× SDS sample buffer. The lysates were separated by SDS-PAGE, and Y1068 EGFR phosphorylation was detected with a phospho-specific antibody (Cell Signaling; no. 2234). The blots were then stripped, and total protein levels and β-actin were detected by immunoblotting with appropriate antibodies against EGFR (Cell Signaling; no. 4267), and β-actin (Cell Signaling; 3700). The immunoblots were developed using enhanced chemiluminescence and imaged with a C400 (Azure Biosystems) digital imager.

Measurement of *R. delemar*-induced host cell damage. *R. delemar*-induced A549 cell damage was quantified using the Pierce LDH assay, with slight modifications to the manufacturer's protocol. Briefly, A549 cells were grown in 96-well tissue culture plates for 18 to 24 h. Cells were then pretreated for 1 h

with gefitinib (25 μM) or cetuximab (25 μg/ml) and infected with 2×10^6 germlings suspended in 150 μl F-12K plus 10% FBS. For controls, host cells were incubated with dimethyl sulfoxide (DMSO) (the solvent used to reconstitute the inhibitor) or 25 μg/ml of mouse IgG antibody in parallel. After 24 h of incubation at 37°C, 50 μl of the cell culture supernatant was collected from uninfected, infected, and fungus-only control wells and transferred to a 96-well plate to assay for LDH activity. Lysis buffer was added to all infected wells, and the mixture was incubated for 45 min at 37°C. After lysis, 50 μl of cell culture supernatant was transferred to a 96-well plate and used for the LDH assay kit per the protocol. LDH release was calculated as follows: % cytotoxicity = [(experimental release − fungal cell spontaneous control − host cell spontaneous control)/(host cell maximum control − fungal cell maximum control − host cell spontaneous control)] × 100. LDH is a cytosolic enzyme but will be released into the cell culture medium upon cell membrane damage. The amount of extracellular LDH is proportional to the amount of cell damage.

Measurement of host cell endocytosis. Twelve-millimeter glass coverslips were seeded with A549 alveolar epithelial cells. Cells were then pretreated for 1 h with gefitinib (25 μM) or cetuximab (25 μg/ml). For controls, host cells will be incubated with DMSO (the solvent used to reconstitute the inhibitor) or 25 μg/ml mouse IgG antibody in parallel. Host cells were then infected with 2×10^5 *R. delemar* spores. After incubation for 3 h, cells were fixed in 3% paraformaldehyde and stained for 1 h with 1% Uvitex, which specifically binds to chitin in the fungal cell wall. After being washed with PBS, coverslips were mounted on a glass slide with a drop of ProLong Gold antifade reagent (Molecular Probes) and sealed. The total number of cell-associated organisms (i.e., fungi adhering to the monolayer) per high-powered field was determined by phase-contrast microscopy. The same field was then examined by epifluorescence microscopy, and the number of brightly fluorescent, uninternalized fungi was determined. The number of endocytosed organisms was calculated by subtracting the number of fluorescent fungi from the total number of visible fungi. At least 400 organisms were counted per treatment group in at least 15 different fields per coverslip. Experiments were performed in duplicate or triplicate on at least two separate days.

Confocal microscopy. The accumulation of epithelial cell EGFR and pEGFR around *R. delemar* was visualized using the Zeiss LSM Duo confocal microscopy system. Twelve-millimeter glass coverslips in 12-well dishes were seeded with A549 alveolar epithelial cells and infected with 2×10^5 *R. delemar* spores. After incubation at 37°C, cells were washed with HBSS and fixed with 3% paraformaldehyde. Cells were blocked and incubated with 1:500 mouse anti-EGFR (Santa Cruz; no. sc-373746) and 1:500 rabbit anti-pEGFR (Cell Signaling; no. 3777). Coverslips were washed and counterstained with 1:500 Alexa Fluor 546-labeled goat anti-mouse IgG and Alexa Fluor 488-labeled goat anti-rabbit IgG. Host cell nuclei were stained with Hoechst 33342 (Thermo Fisher). After washing, coverslips were mounted on a glass slide with ProLong Gold antifade reagent (Molecular Probes) and viewed by z-stacking using the Zeiss LSM Duo confocal microscopy system.

Immunofluorescence of EGFR phosphorylation *in vivo*. CD-1 mice were immunosuppressed with cyclophosphamide (200 mg/kg) and cortisone acetate (500 mg/kg) on day −2 relative to infection. They were inoculated by intratracheal injection of 1.0×10^7 *R. delemar* cells. After 24 h of infection, the mice were sacrificed and the lungs were harvested, snap-frozen in optimal cutting temperature (OCT) compound. Ten-micrometer-thick sections were cut with a cryostat and fixed with cold acetone. Protein phosphorylation was detected as described elsewhere (38, 51). Briefly, the cryosections were rehydrated in PBS and then blocked with 10% bovine serum albumin (BSA). Sections were stained with a phospho-EGFR antibody (Cell Signaling; no. 2234), followed by a secondary antibody. The organisms were stained with calcofluor white (Sigma-Aldrich; no. 18909) and imaged by confocal microscopy.

Statistical analyses. *In vitro* experiments were performed in triplicate on two or three separate days. Data are expressed as the median ± interquartile range. Treatment groups were compared to controls using the Wilcoxon rank sum test. For the murine studies, survival of mice was analyzed using the log rank test, whereas differences in tissue fungal burden were analyzed by the Wilcoxon rank sum test using GraphPad Prism 6. P values of <0.05 were considered significant.

Accession number(s). All of the raw sequencing reads from this study have been submitted to the NCBI sequence read archive (SRA) under BioProject accession no. PRJNA429656 (https://www.ncbi.nlm.nih.gov/bioproject/PRJNA429656). The specific sample accession numbers are presented in Table S1.

SUPPLEMENTAL MATERIAL

Supplemental material for this article may be found at https://doi.org/10.1128/mBio.01384-18.

FIG S1, PDF file, 0.4 MB.
FIG S2, PDF file, 38.1 MB.
FIG S3, PDF file, 0.1 MB.
FIG S4, PDF file, 0.1 MB.
TABLE S1, XLSX file, 0.1 MB.
TABLE S2, XLSX file, 0.2 MB.
TABLE S3, XLSX file, 0.2 MB.
TABLE S4, XLSX file, 0.1 MB.

ACKNOWLEDGMENTS

This project was funded in part with federal funds from the National Institute of Allergy and Infectious Diseases (NIAID), National Institutes of Health (NIH), Department of Health and Human Services, under U19AI110820 to V.M.B., S.G.F., and A.S.I., R01AI063503 to A.S.I., R01AI124566 and R01DE022600 to S.G.F., and K99DE026856 to M.S.

A.S.I. owns shares in Vitalex Biosciences, a start-up company that is developing immunotherapies and diagnostics for mucormycosis. The remaining authors declare no competing interests.

REFERENCES

1. Ribes JA, Vanover-Sams CL, Baker DJ. 2000. Zygomycetes in human disease. Clin Microbiol Rev 13:236–301. https://doi.org/10.1128/CMR.13.2.236-301.2000.
2. Spellberg B, Edwards J, Jr, Ibrahim A. 2005. Novel perspectives on mucormycosis: pathophysiology. presentation, and management. Clin Microbiol Rev 18:556–569. https://doi.org/10.1128/CMR.18.3.556-569.2005.
3. Roden MM, Zaoutis TE, Buchanan WL, Knudsen TA, Sarkisova TA, Schaufele RL, Sein M, Sein T, Chiou CC, Chu JH, Kontoyiannis DP, Walsh TJ. 2005. Epidemiology and outcome of zygomycosis: a review of 929 reported cases. Clin Infect Dis 41:634–653. https://doi.org/10.1086/432579.
4. Ibrahim AS, Kontoyiannis DP. 2013. Update on mucormycosis pathogenesis. Curr Opin Infect Dis 26:508–515. https://doi.org/10.1097/QCO.0000000000000008.
5. Kwon-Chung KJ, Bennett JE. 1992. Medical mycology, p 524–559. Lea & Febiger, Philadelphia, PA.
6. Neblett Fanfair R, Benedict K, Bos J, Bennett SD, Lo YC, Adebanjo T, Etienne K, Deak E, Derado G, Shieh WJ, Drew C, Zaki S, Sugerman D, Gade L, Thompson EH, Sutton DA, Engelthaler DM, Schupp JM, Brandt ME, Harris JR, Lockhart SR, Turabelidze G, Park BJ. 2012. Necrotizing cutaneous mucormycosis after a tornado in Joplin, Missouri, in 2011. N Engl J Med 367:2214–2225. https://doi.org/10.1056/NEJMoa1204781.
7. Andresen D, Donaldson A, Choo L, Knox A, Klaassen M, Ursic C, Vonthethoff L, Krilis S, Konecny P. 2005. Multifocal cutaneous mucormycosis complicating polymicrobial wound infections in a tsunami survivor from Sri Lanka. Lancet 365:876–878. https://doi.org/10.1016/S0140-6736(05)71046-1.
8. Marty FM, Ostrosky-Zeichner L, Cornely OA, Mullane KM, Perfect JR, Thompson GR, III, Alangaden GJ, Brown JM, Fredricks DN, Heinz WJ, Herbrecht R, Klimko N, Klyasova G, Maertens JA, Melinkeri SR, Oren I, Pappas PG, Ráčil Z, Rahav G, Santos R, Schwartz S, Vehreschild JJ, Young JH, Chetchotisakd P, Jaruratanasirikul S, Kanj SS, Engelhardt M, Kaufhold A, Ito M, Lee M, Sasse C, Maher RM, Zeiher B, Vehreschild MJGT, VITAL and FungiScope Mucormycosis Investigators. 2016. Isavuconazole treatment for mucormycosis: a single-arm open-label trial and case-control analysis. Lancet Infect Dis 16:828–837. https://doi.org/10.1016/S1473-3099(16)00071-2.
9. Manesh A, John AO, Mathew B, Varghese L, Rupa V, Zachariah A, Varghese GM. 2016. Posaconazole: an emerging therapeutic option for invasive rhino-orbito-cerebral mucormycosis. Mycoses 59:765–772. https://doi.org/10.1111/myc.12529.
10. Gleissner B, Schilling A, Anagnostopolous I, Siehl I, Thiel E. 2004. Improved outcome of zygomycosis in patients with hematological diseases? Leuk Lymphoma 45:1351–1360. https://doi.org/10.1080/10428190310001653691.
11. Kauffman CA. 2004. Zygomycosis: reemergence of an old pathogen. Clin Infect Dis 39:588–590. https://doi.org/10.1086/422729.
12. Gebremariam T, Liu M, Luo G, Bruno V, Phan QT, Waring AJ, Edwards JE, Jr, Filler SG, Yeaman MR, Ibrahim AS. 2014. CotH3 mediates fungal invasion of host cells during mucormycosis. J Clin Invest 124:237–250. https://doi.org/10.1172/JCI71349.
13. Liu M, Spellberg B, Phan QT, Fu Y, Fu Y, Lee AS, Edwards JE, Jr, Filler SG, Ibrahim AS. 2010. The endothelial cell receptor GRP78 is required for mucormycosis pathogenesis in diabetic mice. J Clin Invest 120:1914–1924. https://doi.org/10.1172/JCI42164.
14. Bruno VM, Shetty AC, Yano J, Fidel PL, Jr, Noverr MC, Peters BM. 2015. Transcriptomic analysis of vulvovaginal candidiasis identifies a role for the NLRP3 inflammasome. mBio 6:e00182-15. https://doi.org/10.1128/mBio.00182-15.
15. Chibucos MC, Soliman S, Gebremariam T, Lee H, Daugherty S, Orvis J, Shetty AC, Crabtree J, Hazen TH, Etienne KA, Kumari P, O'Connor TD, Rasko DA, Filler SG, Fraser CM, Lockhart SR, Skory CD, Ibrahim AS, Bruno VM. 2016. An integrated genomic and transcriptomic survey of mucormycosis-causing fungi. Nat Commun 7:12218. https://doi.org/10.1038/ncomms12218.
16. Liu Y, Shetty AC, Schwartz JA, Bradford LL, Xu W, Phan QT, Kumari P, Mahurkar A, Mitchell AP, Ravel J, Fraser CM, Filler SG, Bruno VM. 2015. New signaling pathways govern the host response to C. albicans infection in various niches. Genome Res 25:679–689. https://doi.org/10.1101/gr.187427.114.
17. Bao W, Jin L, Fu HJ, Shen YN, Lu GX, Mei H, Cao XZ, Wang HS, Liu WD. 2013. Interleukin-22 mediates early host defense against Rhizomucor pusilluscan pathogens. PLoS One 8:e65065. https://doi.org/10.1371/journal.pone.0065065.
18. Flemming A. 2017. Antifungals: JNK inhibitors boost antifungal immunity. Nat Rev Drug Discov 16:163. https://doi.org/10.1038/nrd.2017.29.
19. Gavino C, Hamel N, Zeng JB, Legault C, Guiot MC, Chankowsky J, Lejtenyi D, Lemire M, Alarie I, Dufresne S, Boursiquot JN, McIntosh F, Langelier M, Behr MA, Sheppard DC, Foulkes WD, Vinh DC. 2016. Impaired RASGRF1/ERK-mediated GM-CSF response characterizes CARD9 deficiency in French-Canadians. J Allergy Clin Immunol 137:1178–1188.e7. https://doi.org/10.1016/j.jaci.2015.09.016.
20. Horng T, Medzhitov R. 2001. Drosophila MyD88 is an adapter in the Toll signaling pathway. Proc Natl Acad Sci U S A 98:12654–12658. https://doi.org/10.1073/pnas.231471798.
21. Marr KA, Balajee SA, Hawn TR, Ozinsky A, Pham U, Akira S, Aderem A, Liles WC. 2003. Differential role of MyD88 in macrophage-mediated responses to opportunistic fungal pathogens. Infect Immun 71:5280–5286. https://doi.org/10.1128/IAI.71.9.5280-5286.2003.
22. Moyes DL, Runglall M, Murciano C, Shen C, Nayar D, Thavaraj S, Kohli A, Islam A, Mora-Montes H, Challacombe SJ, Naglik JR. 2010. A biphasic innate immune MAPK response discriminates between the yeast and hyphal forms of Candida albicans in epithelial cells. Cell Host Microbe 8:225–235. https://doi.org/10.1016/j.chom.2010.08.002.
23. Wang J, Gigliotti F, Bhagwat SP, Maggirwar SB, Wright TW. 2007. Pneumocystis stimulates MCP-1 production by alveolar epithelial cells through a JNK-dependent mechanism. Am J Physiol Lung Cell Mol Physiol 292:L1495–L1505. https://doi.org/10.1152/ajplung.00452.2006.
24. Wozniok I, Hornbach A, Schmitt C, Frosch M, Einsele H, Hube B, Löffler J, Kurzai O. 2008. Induction of ERK-kinase signalling triggers morphotype-specific killing of Candida albicans filaments by human neutrophils. Cell Microbiol 10:807–820. https://doi.org/10.1111/j.1462-5822.2007.01086.x.
25. Buscaglia LE, Li Y. 2011. Apoptosis and the target genes of microRNA-21. Chin J Cancer 30:371–380. https://doi.org/10.5732/cjc.30.0371.
26. Feng YH, Tsao CJ. 2016. Emerging role of microRNA-21 in cancer. Biomed Rep 5:395–402. https://doi.org/10.3892/br.2016.747.
27. Li Y, Zhang J, Lei Y, Lyu L, Zuo R, Chen T. 2017. MicroRNA-21 in skin fibrosis: potential for diagnosis and treatment. Mol Diagn Ther 21:633–642. https://doi.org/10.1007/s40291-017-0294-8.
28. Sekar D, Shilpa BR, Das AJ. 2017. Relevance of microRNA 21 in different types of hypertension. Curr Hypertens Rep 19:57. https://doi.org/10.1007/s11906-017-0752-z.
29. Sekar D, Venugopal B, Sekar P, Ramalingam K. 2016. Role of microRNA 21 in diabetes and associated/related diseases. Gene 582:14–18. https://doi.org/10.1016/j.gene.2016.01.039.
30. Wang S, Wan X, Ruan Q. 2016. The microRNA-21 in autoimmune diseases. Int J Mol Sci 17:E864. https://doi.org/10.3390/ijms17060864.

31. Seike M, Goto A, Okano T, Bowman ED, Schetter AJ, Horikawa I, Mathe EA, Jen J, Yang P, Sugimura H, Gemma A, Kudoh S, Croce CM, Harris CC. 2009. MiR-21 is an EGFR-regulated anti-apoptotic factor in lung cancer in never-smokers. Proc Natl Acad Sci U S A 106:12085–12090. https://doi.org/10.1073/pnas.0905234106.
32. Decker SJ. 1993. Transmembrane signaling by epidermal growth factor receptors lacking autophosphorylation sites. J Biol Chem 268:9176–9179.
33. Ho J, Moyes DL, Tavassoli M, Naglik JR. 2017. The role of ErbB receptors in infection. Trends Microbiol 25:942–952. https://doi.org/10.1016/j.tim.2017.04.009.
34. Zhu W, Phan QT, Boontheung P, Solis NV, Loo JA, Filler SG. 2012. EGFR and HER2 receptor kinase signaling mediate epithelial cell invasion by Candida albicans during oropharyngeal infection. Proc Natl Acad Sci U S A 109:14194–14199. https://doi.org/10.1073/pnas.1117676109.
35. Wang X, Maruvada R, Morris AJ, Liu JO, Wolfgang MJ, Baek DJ, Bittman R, Kim KS. 2016. Sphingosine 1-phosphate activation of EGFR as a novel target for meningitic Escherichia coli penetration of the blood-brain barrier. PLoS Pathog 12:e1005926. https://doi.org/10.1371/journal.ppat.1005926.
36. Vincenzi B, Zoccoli A, Pantano F, Venditti O, Galluzzo S. 2010. Cetuximab: from bench to bedside. Curr Cancer Drug Targets 10:80–95. https://doi.org/10.2174/156800910790980241.
37. Ibrahim AS, Spellberg B, Avanessian V, Fu Y, Edwards JE, Jr. 2005. Rhizopus oryzae adheres to, is phagocytosed by, and damages endothelial cells in vitro. Infect Immun 73:778–783. https://doi.org/10.1128/IAI.73.2.778-783.2005.
38. Solis NV, Swidergall M, Bruno VM, Gaffen SL, Filler SG. 2017. The aryl hydrocarbon receptor governs epithelial cell invasion during oropharyngeal candidiasis. mBio 8:e00025-17. https://doi.org/10.1128/mBio.00025-17.
39. Miettinen PJ, Berger JE, Meneses J, Phung Y, Pedersen RA, Werb Z, Derynck R. 1995. Epithelial immaturity and multiorgan failure in mice lacking epidermal growth factor receptor. Nature 376:337–341. https://doi.org/10.1038/376337a0.
40. Luo G, Gebremariam T, Lee H, French SW, Wiederhold NP, Patterson TF, Filler SG, Ibrahim AS. 2013. Efficacy of liposomal amphotericin B and posaconazole in intratracheal models of murine mucormycosis. Antimicrob Agents Chemother 57:3340–3347. https://doi.org/10.1128/AAC.00313-13.
41. Lynch TJ, Bell DW, Sordella R, Gurubhagavatula S, Okimoto RA, Brannigan BW, Harris PL, Haserlat SM, Supko JG, Haluska FG, Louis DN, Christiani DC, Settleman J, Haber DA. 2004. Activating mutations in the epidermal growth factor receptor underlying responsiveness of non-small-cell lung cancer to gefitinib. N Engl J Med 350:2129–2139. https://doi.org/10.1056/NEJMoa040938.
42. Schneider MR, Wolf E. 2009. The epidermal growth factor receptor ligands at a glance. J Cell Physiol 218:460–466. https://doi.org/10.1002/jcp.21635.
43. Plissonnier ML, Lahlali T, Michelet M, Lebossé F, Cottarel J, Beer M, Neveu G, Durantel D, Bartosch B, Accardi R, Clément S, Paradisi A, Devouassoux-Shisheboran M, Einav S, Mehlen P, Zoulim F, Parent R. 2016. Epidermal growth factor receptor-dependent mutual amplification between Netrin-1 and the hepatitis C virus. PLoS Biol 14:e1002421. https://doi.org/10.1371/journal.pbio.1002421.
44. Stindt S, Cebula P, Albrecht U, Keitel V, Schulte am Esch J, Knoefel WT, Bartenschlager R, Häussinger D, Bode JG. 2016. Hepatitis C virus activates a neuregulin-driven circuit to modify surface expression of growth factor receptors of the ErbB family. PLoS One 11:e0148711. https://doi.org/10.1371/journal.pone.0148711.
45. Krause-Gruszczynska M, Boehm M, Rohde M, Tegtmeyer N, Takahashi S, Buday L, Oyarzabal OA, Backert S. 2011. The signaling pathway of Campylobacter jejuni-induced Cdc42 activation: role of fibronectin, integrin beta1, tyrosine kinases and guanine exchange factor Vav2. Cell Commun Signal 9:32. https://doi.org/10.1186/1478-811X-9-32.
46. Press MF, Lenz HJ. 2007. EGFR, HER2 and VEGF pathways: validated targets for cancer treatment. Drugs 67:2045–2075. https://doi.org/10.2165/00003495-200767140-00006.
47. Ibrahim AS, Bowman JC, Avanessian V, Brown K, Spellberg B, Edwards JE, Jr, Douglas CM. 2005. Caspofungin inhibits Rhizopus oryzae 1,3-beta-D-glucan synthase, lowers burden in brain measured by quantitative PCR, and improves survival at a low but not a high dose during murine disseminated zygomycosis. Antimicrob Agents Chemother 49:721–727. https://doi.org/10.1128/AAC.49.2.721-727.2005.
48. Kim D, Pertea G, Trapnell C, Pimentel H, Kelley R, Salzberg SL. 2013. TopHat2: accurate alignment of transcriptomes in the presence of insertions, deletions and gene fusions. Genome Biol 14:R36. https://doi.org/10.1186/gb-2013-14-4-r36.
49. Robinson MD, McCarthy DJ, Smyth GK. 2010. edgeR: a Bioconductor package for differential expression analysis of digital gene expression data. Bioinformatics 26:139–140. https://doi.org/10.1093/bioinformatics/btp616.
50. Liu H, Lee MJ, Solis NV, Phan QT, Swidergall M, Ralph B, Ibrahim AS, Sheppard DC, Filler SG. 2016. Aspergillus fumigatus CalA binds to integrin alpha5beta1 and mediates host cell invasion. Nat Microbiol 2:16211. https://doi.org/10.1038/nmicrobiol.2016.211.
51. Swidergall M, Solis NV, Lionakis MS, Filler SG. 2018. EphA2 is an epithelial cell pattern recognition receptor for fungal beta-glucans. Nat Microbiol 3:53–61. https://doi.org/10.1038/s41564-017-0059-5.